Letter

Entropy production limits all fluctuation oscillations

Naoto Shiraishi
Faculty of arts and sciences, University of Tokyo, 3-8-1 Komaba, Meguro-ku, Tokyo, 153-8902, Japan

(Received 4 May 2023; accepted 3 October 2023; published 27 October 2023)

The oscillation of fluctuation with two state observables is investigated. Following the idea of Ohga *et al.* [Phys. Rev. Lett. **131**, 077101 (2023)], we find that the fluctuation oscillation relative to their autocorrelations is bounded from above by the entropy production per characteristic maximum oscillation time. Our result applies to a variety of systems including Langevin systems, chemical reaction systems, and macroscopic systems. In addition, our bound consists of experimentally tractable quantities, which enables us to examine our inequality experimentally.

DOI: 10.1103/PhysRevE.108.L042103

Introduction. Entropy production plays a pivotal role in nonequilibrium statistical mechanics, quantifying the degree of the thermodynamic irreversibility of processes. The celebrated fluctuation theorem [1–5] and its variants [6–10] clearly show the mathematical structure of the thermodynamic irreversibility in an equality form. In addition, entropy production satisfies not only equalities but also various inequalities as the upper bounds of quantities [11]. One famous example is the classical speed limit inequalities [12–15] and the trade-off relation between the efficiency and power of heat engines [16,17]. Here, entropy production bounds the speed of processes: A quick process should accompany much entropy production. The thermodynamic uncertainty relation [18–24] is another example, where entropy production bounds the relative fluctuation of general currents. Furthermore, entropy production serves as a restriction on possible paths in state space observed in relaxation processes [25,26].

We investigate this direction further in the context of oscillation phenomena. Our main subject in this Letter is the fluctuation oscillation in the stationary distribution with two state variables a and b defined as

$$\alpha_{ab} := \tfrac{1}{2}\langle a\dot{b} - b\dot{a}\rangle, \tag{1}$$

with time derivative $\dot{a} := \lim_{\Delta t\to 0}[a(t+\Delta t) - a(t)]/\Delta t$, which is also called the *irreversible circulation of fluctuation* [27] and *asymmetry of cross-correlation* [28] (see Fig. 1). The fluctuation oscillation α_{ab} can be interpreted as the angular momentum in the a-b plane, and therefore α_{ab} quantifies the strength of rotation in terms of a and b. Since the stationary fluctuation oscillation takes a nonzero value only at nonequilibrium stationary states, this quantity is sometimes regarded as the characterization of thermodynamics irreversibility [27] (i.e., far from equilibrium).

Oscillation phenomena including chemical oscillations were investigated in the field of nonlinear physics [29–31], and have attracted renewed interest from the viewpoint of stochastic thermodynamics [32–42]. Recently, interesting progress was provided by Ohga *et al.* [28], which proposes a bound on fluctuation oscillation relative to autocorrelation by using the maximum cycle affinity in the transition network. This bound builds a bridge between fluctuation oscillation and some thermodynamic quantity. However, the maximum cycle affinity of systems with multiple cycles is sometimes not easy to measure in experiments. In particular, the connection to entropy production has not yet been addressed.

In this Letter, we prove the upper bounds on fluctuation oscillation by entropy production per characteristic time length of oscillation. Our result clearly shows that a long-lived oscillation inevitably accompanies much dissipation. Employing the geometric interpretation proposed by Ohga *et al.* [28], we can derive our results transparently. Our result has wide applicability from particle systems in continuous space to chemical reaction systems. Another advantage of our result is that the inequality consists only of the fluctuation oscillation, autocorrelation, the operator norm of observables, and the entropy production rate, all of which are tractable in various experiments. Thus, our relation serves as a good stage to test the thermodynamic properties in oscillation phenomena.

Setup and main result. We consider a Markov jump process on discrete states, whose time evolution is given by the following master equation:

$$\frac{d}{dt}p_i = \sum_j R_{ij}p_j. \tag{2}$$

Here, p_i is the probability distribution of state i, and R is a transition matrix satisfying non-negativity $R_{ij} \geqslant 0\ (i \neq j)$ and the normalization condition $\sum_i R_{ij} = 0$. We assume the local detailed-balance condition, with which the stationary entropy production rate $\dot{\sigma}$ is expressed as

$$\dot{\sigma} = \sum_{i,j} R_{ij}p_j^{\mathrm{ss}} \ln \frac{R_{ij}p_j^{\mathrm{ss}}}{R_{ji}p_i^{\mathrm{ss}}}, \tag{3}$$

with the stationary distribution p^{ss}.

The stationary fluctuation oscillation with a and b can be expressed as

$$\alpha_{ab} = \frac{1}{2}\sum_{i,j}(a_jb_i - a_ib_j)R_{ij}p_j^{\mathrm{ss}} = \frac{1}{2}\sum_{(i,j)}(a_jb_i - a_ib_j)J_{ij}^{\mathrm{ss}}, \tag{4}$$

where $J_{ij}^{\mathrm{ss}} := R_{ij}p_j^{\mathrm{ss}} - R_{ji}p_i^{\mathrm{ss}}$ is the stationary current between j and i, and $\sum_{(i,j)}$ represents the sum over a pair of i and

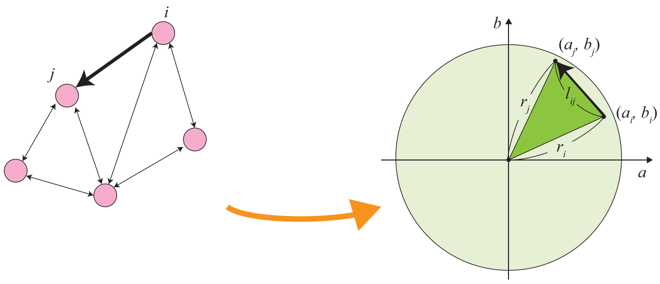

FIG. 1. An example of state space and its geometric interpretation of fluctuation oscillation and other quantities in the *a*-*b* space. Here, *a* and *b* are two observables which take values a_i and b_i at state i. The terms in the fluctuation oscillation $\alpha_{ab} = \langle a\dot{b} - b\dot{a}\rangle$ can be interpreted as the area with dark green (with transition probability). We also express $\ell_{ij} = \sqrt{(a_i - a_j)^2 + (b_i - b_j)^2}$ and $r_i = \sqrt{a_i^2 + b_i^2}$. All points (a_i, b_i) are in the circle with diameter $\|\sqrt{a^2 + b^2}\| := \max_i \sqrt{a_i^2 + b_i^2}$ drawn in light green.

j (i.e., we take only one of ij and ji). We introduce the autocorrelation of a defined as

$$D_a := -\langle a\dot{a}\rangle = \frac{1}{2}\sum_{i,j}(a_i - a_j)^2 R_{ij} p_j^{\rm ss}, \tag{5}$$

which quantifies the speed of decay of a since D_a is the half of $d(a^2)/dt$. Here, $\dot{a}$ is defined in a manner presented below Eq. (1). We normalize the fluctuation oscillation α_{ab} by the average of autocorrelations of a and b; $(D_a + D_b)/2$.

Below we present two upper bounds on the normalized fluctuation oscillation $2\alpha_{ab}/(D_a + D_b)$ with the stationary entropy production rate $\dot{\sigma}$ relative to the maximum speed of oscillation. Two inequalities employ different measures of the speed of oscillation. In the first inequality, we characterize the speed of oscillation by the fluctuation oscillation divided by the area of the circle with a diameter equal to the maximum of $\sqrt{a^2 + b^2}$. The obtained bound is

$$\frac{2|\alpha_{ab}|}{D_a + D_b} \leqslant \frac{\dot{\sigma}}{2\pi\, w_{\rm osci}}, \tag{6}$$

which is our first main result. Here, $w_{\rm osci}$ is defined as

$$w_{\rm osci} := \frac{|\alpha_{ab}|}{\pi\,\|a^2 + b^2\|}, \tag{7}$$

with the operator norm $\|a^2 + b^2\| = \max_i[a_i^2 + b_i^2]$. The denominator represents the area of the circle with diameter $\|\sqrt{a^2 + b^2}\|$. Since α_{ab} can be regarded as the area of a circular sector (see Fig. 1) with a diameter less than $\|\sqrt{a^2 + b^2}\|$, we can see $w_{\rm osci}$ as the maximum angular velocity. We remark that in the definition of $w_{\rm osci}$ we can replace the position of the origin to (a', b') and define as $w_{\rm osci} = |\alpha_{ab}|/\pi\,\|(a - a')^2 + (b - b')^2\|$, with which we can derive the same bound (6).

The idea behind the second inequality is closer to that shown in Ohga *et al.* [28], which relies heavily on the isoperimetric inequality. From the viewpoint of the isoperimetric inequality, the area of a circle is connected to the square of the perimeter of the circle. In this line, we claim our second main result:

$$\frac{2|\alpha_{ab}|}{D_a + D_b} \leqslant \frac{\dot{\sigma}}{2\pi\, v_{\rm osci}}. \tag{8}$$

Here, $v_{\rm osci}$ is defined as

$$v_{\rm osci} := \frac{4\pi\,|\alpha_{ab}|}{\left(\max_{C\in\mathcal{C}_{\rm ucd}} \ell_C\right)^2}, \tag{9}$$

where $\ell_C := \sum_{(i,j)\in C}\sqrt{(a_i - a_j)^2 + (b_i - b_j)^2}$ is the length of cycle C in the *a*-*b* plane, and $\mathcal{C}_{\rm ucd}$ is a set of cycles in the uniform cycle decomposition [43]. The uniform cycle decomposition is a cycle decomposition [44] such that the direction of cycles and that of current coincide on any edge, whose existence is established. As mentioned above, $\ell_C^2/4\pi$ corresponds to the area bounded by C.

These two inequalities clearly show that possible fluctuation oscillation is bounded above by the dissipation. Some arguments shown in the remainder suggest that the first inequality (6) is more useful in several places than the second one (8). We remark that the denominator of $w_{\rm osci}$ depends only on the state variables a and b, and that of $v_{\rm osci}$ depends only on a, b, the topology of the transition map, and the form of the uniform cycle decomposition, and the effects of the transition rates and the stationary distribution are only seen through the uniform cycle decomposition.

Comparison with previous theoretical works. Before going to the proof of these bounds, we here discuss their physical implications and compare our bounds with other relevant works.

We first remark on the connection to the response theory. Consider a macroscopic stationary system with a and b as conserved quantities supplied from reservoirs. We apply the system size expansion [27,45], which is an established method to evaluate small fluctuations around the averaged macroscopic dynamics by the Kramers-Moyal expansion. In the lowest order, the fluctuation of observables in the vector form $\boldsymbol{X} = (\Delta a, \Delta b)^\top$ obeys a stochastic equation $\dot{\boldsymbol{X}} = L\boldsymbol{X} + \boldsymbol{\xi}$, where L is the response matrix and $\boldsymbol{\xi}$ is the noise term. Around an equilibrium state, the celebrated Onsager reciprocity theorem states that two off-diagonal elements are equal, $L_{12} = L_{21}$, which follows from the microscopic reversibility of dynamics. In contrast, around a nonequilibrium stationary state, the Onsager reciprocity relation no longer holds, $L_{12} \neq L_{21}$, and its discrepancy is known to be equal to the fluctuation oscillation (the irreversible circulation of fluctuation): $(L_{ab} - L_{ba})/2 = \alpha_{ab}$ [27]. Thus, our results also serve as a bound on the antisymmetric part of the response matrix by entropy production, which is sometimes referred to as a characterization of microscopic irreversibility (the degree of nonequilibriumness).

A further implication is seen in the bifurcation phenomena. When bifurcation occurs, the fluctuation of an observable (D_a or D_b) diverges, and in some cases, the oscillation fluctuation (α_{ab}) also diverges simultaneously, which are called soft-mode instability and hard-mode instability, respectively [30]. Since the entropy production rate $\dot{\sigma}$ does not diverge at the bifurcation point, our results can also be read as a bound on the speed of divergence of these two instabilities in terms of entropy production.

Next, we compare our results with the conjecture raised by Oberreiter *et al.* [41], which conjectures that the second largest eigenvalue λ of the transition matrix R satisfies $({\rm Im}\,\lambda)^2/{\rm Re}\,\lambda \leqslant \dot{\sigma}$. To compare our results, we introduce the

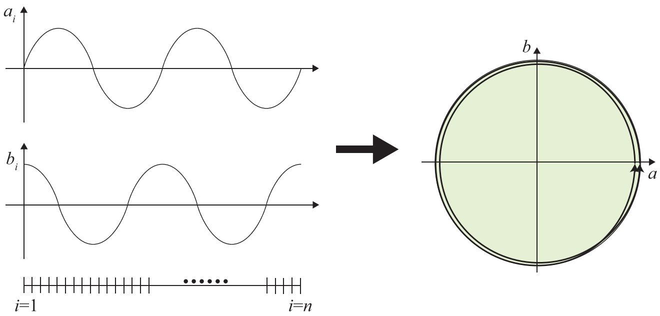

FIG. 2. An example of a_i and b_i in a unicyclic system. By taking the $n \to \infty$ limit, the point (a_i, b_i) moves on the circumference of the light green circle. In this case, the point in a-b space rotates twice per single period.

corresponding eigenvector $\boldsymbol{v}$ normalized as $\sum_i |v_i|^2/p_i^{\rm ss} = 1$. By setting $a_i = {\rm Re}\, v_i/p_i^{\rm ss}$ and $b_i = {\rm Im}\, v_i/p_i^{\rm ss}$ and comparing the relation $\lambda \boldsymbol{v}^\dagger \boldsymbol{v} = \boldsymbol{v}^\dagger R \boldsymbol{v}$, the oscillation fluctuation and the autocorrelation become equivalent to the real and the imaginary part of the second largest eigenvalue: ${\rm Im}\, \lambda = \alpha_{ab}$ and ${\rm Re}\, \lambda = D_a + D_b$ [28]. However, to proceed to the above conjecture or a similar relation from our bounds, we need to evaluate the eigenvector $\boldsymbol{v}$, which appears in the form of $\|a^2 + b^2\|$ in the case of Eq. (6). At present, we do not have good tools to examine this eigenvector in detail, which is left as a future problem.

We finally compare our results to the relations shown in Ohga *et al.* [28]. In both inequalities, the fluctuation oscillation relative to the autocorrelation is bounded from above. The difference lies in the fact that the bound shown in Ref. [28] employs the maximum cycle affinity as a thermodynamic quantity, while our bounds employ an entropy production rate. To compute the cycle affinity, we need detailed information on the system. In contrast, the stationary entropy production rate depends only on stationary currents of conserved quantities such as heat currents and particle currents. These quantities can be measured not only by tracking microscopic trajectories but also by measuring the total change in energy or number of particles of baths. In particular, Eq. (6) connects the oscillation fluctuation, autocorrelation, and entropy production rate directly. We expect that the experimental verification of Eq. (6) is tractable in several micro- and mesoscale stochastic systems and chemical systems. Candidates are KaiC proteins [46], the genetic repressilator [47], and many other oscillating biochemical system (see Ref. [32] for further examples).

Example: Unicyclic system. To shed light on the power of our inequalities, we apply them to the simplest setup, a uniform unicyclic system with n states, which is analyzed in Ref. [41]. We set the transition rates as $R_{i+1,i} = ke^{\beta F/n}$ and $R_{i,i+1} = k$, where we identify state $n+1$ with state 1. The stationary entropy production rate is computed as

$$\dot{\sigma} = k(e^{\beta F/n} - 1)\frac{\beta F}{n}. \tag{10}$$

We set two observables as $a_i = \sin \omega i$ and $b_i = \cos \omega i$ with $\omega = 2\pi m/n$, where m is a natural number (the case of $m = 2$ is drawn in Fig. 2). Then, both the fluctuation oscillation and the autocorrelation are calculated as $\alpha_{ab} = \frac{1}{2}k(e^{\beta F/n} - 1) \sin \omega$ and $D_a = D_b = k(e^{\beta F/n} + 1)\sin^2(\omega/2)$, whose ratio behaves as

$$\frac{2|\alpha_{ab}|}{D_a + D_b} = \frac{\sin \omega \tanh \frac{\beta F}{2n}}{2\sin^2(\omega/2)} \simeq \frac{\beta F}{2\pi m}, \tag{11}$$

where the last approximation is valid under the large n situation. In addition, by noting $\|a^2 + b^2\| = 1$ and $\ell_C = 2n\sin(\pi m/n)$, two definitions of a characteristic maximum speed of oscillation are calculated as $w_{\rm osci} = |\alpha_{ab}|/\pi = \frac{1}{2}k(e^{\beta F/n} - 1)\sin(2\pi m/n)/\pi$ and $v_{\rm osci} = 4\pi|\alpha_{ab}|/\ell_C^2 = \frac{1}{2}k(e^{\beta F/n} - 1)\pi \sin(2\pi m/n)/n^2 \sin^2(\pi m/n)$. Thus, the right-hand sides of the two inequalities (6) and (8) read

$$\frac{\dot{\sigma}}{2\pi w_{\rm osci}} = \frac{\beta F}{n \sin \frac{2\pi m}{n}} \simeq \frac{\beta F}{2\pi m}, \tag{12}$$

$$\frac{\dot{\sigma}}{2\pi v_{\rm osci}} = \frac{\beta F n^2 \sin^2 \frac{\pi m}{n}}{\pi^2 \sin \frac{2\pi m}{n}} \simeq \frac{\beta F m}{2\pi}. \tag{13}$$

Comparing Eq. (11), we see that Eq. (6) achieves its equality for any m, while Eq. (8) does only when $m = 1$ and it is a loose bound by m^2 for $m \geqslant 2$. This difference comes from the looseness of the isoperimetric inequality when the winding number of the polylateral around the center is not one.

Other possible applications. We here briefly draw other possible applications. One important application is to two-dimensional Langevin systems in a confined region with rotational force. This is straightforward by following a standard method [11,16] that we first discretize the space and then take the continuous limit. We note that the quantities in Eq. (6), the fluctuation oscillation, autocorrelation, entropy production rate, and the norm of $a^2 + b^2$, do not diverge in this limit.

Another important application is to chemical reaction systems. Some chemical systems including the Brusselator model show a nonequilibrium phase transition to a coherent oscillation phase [29]. From a microscopic perspective, the state of the system is a pair of particle numbers, and transition rates between two states are given from a chemical reaction network. If a chemical system has two species X and Y, for example, the microscopic state is given by (n_X, n_Y). An example of the state space (a reversible Brusselator model) is shown in Fig. 3. A proper macroscopic limit recovers its deterministic time evolution. Setting $a = n_X$ and $b = n_Y$, we can examine the magnitude of oscillation in the n_X-n_Y plane in terms of autocorrelation, entropy production rate, and the maximum number of species, which is well defined under a proper cutoff.

Proofs of Eqs. (6) and (8). We derive two inequalities by replacing the entropy production rate $\dot{\sigma}$ with the *pseudoentropy production rate* [11,22]

$$\dot{\Pi} := \sum_{(i,j)} \frac{\left(R_{ij}p_j^{\rm ss} - R_{ji}p_i^{\rm ss}\right)^2}{R_{ij}p_j^{\rm ss} + R_{ji}p_i^{\rm ss}} = \sum_{(i,j)} \frac{J_{ij}^2}{A_{ij}}. \tag{14}$$

Here, we defined the local activity, or traffic, in the stationary state as $A_{ij} = R_{ij}p_j^{\rm ss} + R_{ji}p_i^{\rm ss}$, which quantifies the frequency of jumps between i and j. Noting $\dot{\Pi} \leqslant \dot{\sigma}$, we confirm that proving inequalities with $\dot{\Pi}$ suffices for our purpose.

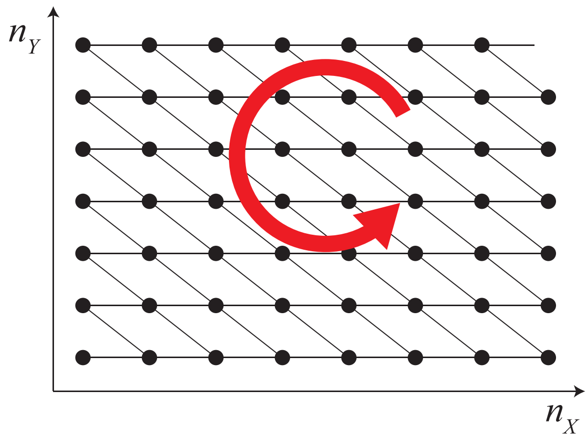

FIG. 3. An example of the state space of a chemical reaction model, the reversible Brusselator model: $A \leftrightarrow X$, $2X + Y \leftrightarrow 3X$, $B + X \leftrightarrow Y + D$, $X \leftrightarrow E$. A single state is represented by a single vertex (n_X, n_Y), and a state can jump to another state connected by an edge in a single transition. We can expect oscillation (rotational flow) as the red arrow in some parameter regime, which can be captured by our bound (6) with a proper cutoff.

We employ a geometric interpretation with the *a*-*b* plane (see Fig. 1). We introduce two distances One is between two states i and j and the other is from the origin, denoted by $\ell_{ij} := \sqrt{(a_i - a_j)^2 + (b_i - b_j)^2}$ and $r_i := \sqrt{a_i^2 + b_i^2}$, respectively. The oriented area of the triangle with i, j and the origin, with edges ℓ_{ij}, r_i, and r_j, is expressed as $S_{ij} := \frac{1}{2}(a_j b_i - a_i b_j)$. Using these quantities, the averaged autocorrelation $(D_a + D_b)/2$, which appears on the left-hand side of the main results as its denominator, is written as

$$\frac{D_a + D_b}{2} = \frac{1}{2} \sum_{(i,j)} A_{ij} \ell_{ij}^2. \tag{15}$$

A key fact to derive Eq. (6) is that the oriented area of a triangle is always less than half of the product of two edges,

$$S_{ij} \leqslant \tfrac{1}{2} \ell_{ij} r_i \leqslant \tfrac{1}{2} \ell_{ij} r_{\max}, \tag{16}$$

where $r_{\max} := \max_i r_i = \|\sqrt{a_i^2 + b_i^2}\|$ is the maximum distance of point (a_i, b_i) from the origin. Using this relation and the Schwarz inequality, we have Eq. (6):

$$\begin{aligned} \frac{2|\alpha_{ab}^2|}{D_a + D_b} &= \frac{2\left(\sum_{(i,j)} J_{ij} S_{ij}\right)^2}{\sum_{(i,j)} A_{ij} \ell_{ij}^2} \leqslant \frac{r_{\max}^2}{2} \frac{\left(\sum_{(i,j)} J_{ij} \ell_{ij}\right)^2}{\sum_{(i,j)} A_{ij} \ell_{ij}^2} \\ &\leqslant \frac{r_{\max}^2}{2} \sum_{(i,j)} \frac{J_{ij}^2}{A_{ij}} = \frac{r_{\max}^2}{2} \dot{\Pi} \leqslant \frac{r_{\max}^2}{2} \dot{\sigma}. \end{aligned} \tag{17}$$

Here, we set the direction of edge ij such that J_{ij} is non-negative.

We next derive Eq. (8), which requires a more complicated evaluation. We consider a uniform cycle decomposition of current J with cycle set $\mathcal{C}$. With this decomposition, we can set the direction of all cycles such that the current J_C with any cycle C is non-negative. We denote the nth state in cycle C by i_n^C, and define the *length* of cycle C as $\ell_C := \sum_{n=1}^{N_C} \ell_{i_{n+1}^C i_n^C}$. Here, N_C is the number of states in cycle C and we identify $i_{N_C+1}^C = i_1^C$.

Now, we employ the discrete isoperimetric inequality [28,48]. The discrete isoperimetric inequality for N_C lateral in the *a*-*b* plane with the nth vertex $(a_{i_n^C}, b_{i_n^C})$ reads

$$\left(4N_C \tan\frac{\pi}{N_C}\right)\left|\sum_{n=1}^{N_C} S_{i_{n+1}^C i_n^C}\right| \leqslant \ell_C^2. \tag{18}$$

Employing this relation, the fluctuation oscillation is evaluated as

$$\begin{aligned} \alpha_{ab} &= \sum_C J_C \sum_{n=1}^{N_C} S_{i_{n+1}^C i_n^C} \leqslant \sum_C \frac{J_C}{4N_C \tan\frac{\pi}{N_C}} \ell_C^2 \\ &\leqslant \frac{\max_C \ell_C}{4\pi} \sum_C J_C \ell_C = \frac{\max_C \ell_C}{4\pi} \sum_{(i,j)} J_{ij} \ell_{ij}, \end{aligned} \tag{19}$$

where we used $a \tan\frac{\pi}{a} \geqslant \pi$ for $0 < a < \frac{1}{2}$. Following a similar transformation to Eq. (17), we arrive at Eq. (8).

Discussion. We derived thermodynamic bounds on fluctuation oscillation in a simple form, which is easy to address experimentally. Our result has wide applicability, from particle systems in continuous space to chemical reaction systems, which is another advantage of our bound.

One may expect to extend this result to underdamped systems (systems with inertia). However, unfortunately, a naive extension faces a simple counterexample. A closed Hamilton dynamics has finite fluctuation oscillation in general while it accompanies no entropy production, which always violates inequalities in the form of Eqs. (6) and (8). Thus, to extend the obtained bound on fluctuation oscillation to diffusive systems, we need some restriction on observables or addition of terms.

Another possible extension one may hope for is that the operator norm $\|\sqrt{a^2 + b^2}\|$ in Eq. (6) can be replaced by the stationary average $\langle\sqrt{a^2 + b^2}\rangle$ or a similar quantity. However, adopting an approach similar to ours, it appears not easy to derive such a relation. On the left-hand side of Eq. (6), both the numerator (α_{ab}) and the denominator (D_a and D_b) employ the information of the stationary distribution p^{ss}. This is also true for the right-hand side: Both the numerator ($\dot{\sigma}$) and the denominator (α_{ab}) employ the information of the stationary distribution p^{ss}. Thus, there is no room for other quantities including $\|a^2 + b^2\|$ to employ the information of the stationary distribution p^{ss}.

Acknowledgment. The author is supported by JSPS KAKENHI Grants-in-Aid for Early-Career Scientists Grant No. JP19K14615.

[1] D. J. Evans, E. G. D. Cohen, and G. P. Morriss, Probability of second law violations in shearing steady states, Phys. Rev. Lett. **71**, 2401 (1993).

[2] G. Gallavotti and E. G. D. Cohen, Dynamical ensembles in nonequilibrium statistical mechanics, Phys. Rev. Lett. **74**, 2694 (1995).

[3] J. Kurchan, Fluctuation theorem for stochastic dynamics, J. Phys. A: Math. Gen. **31**, 3719 (1998).

[4] C. Maes, The fluctuation theorem as a Gibbs property, J. Stat. Phys. **95**, 367 (1999).

[5] C. Jarzynski, Hamiltonian derivation of a detailed fluctuation theorem, J. Stat. Phys. **98**, 77 (2000).

[6] C. Jarzynski, Nonequilibrium equality for free energy differences, Phys. Rev. Lett. **78**, 2690 (1997).

[7] T. Hatano and S.-I. Sasa, Steady-state thermodynamics of Langevin systems, Phys. Rev. Lett. **86**, 3463 (2001).

[8] T. Sagawa and M. Ueda, Fluctuation theorem with information exchange: Role of correlations in stochastic thermodynamics, Phys. Rev. Lett. **109**, 180602 (2012).

[9] N. Shiraishi and T. Sagawa, Fluctuation theorem for partially masked nonequilibrium dynamics, Phys. Rev. E **91**, 012130 (2015).

[10] M. Polettini and M. Esposito, Effective thermodynamics for a marginal observer, Phys. Rev. Lett. **119**, 240601 (2017).

[11] N. Shiraishi, *An Introduction to Stochastic Thermodynamics* (Springer, Berlin, 2023).

[12] N. Shiraishi, K. Funo, and K. Saito, Speed limit for classical stochastic processes, Phys. Rev. Lett. **121**, 070601 (2018).

[13] V. T. Vo, T. Van Vu, and Y. Hasegawa, Unified approach to classical speed limit and thermodynamic uncertainty relation, Phys. Rev. E **102**, 062132 (2020).

[14] A. Dechant, Minimum entropy production, detailed balance and Wasserstein distance for continuous-time Markov processes, J. Phys. A: Math. Theor. **55**, 094001 (2022).

[15] T. Van Vu and K. Saito, Thermodynamic unification of optimal transport: Thermodynamic uncertainty relation, minimum dissipation, and thermodynamic speed limits, Phys. Rev. X **13**, 011013 (2023).

[16] N. Shiraishi, K. Saito, and H. Tasaki, Universal trade-off relation between power and efficiency for heat engines, Phys. Rev. Lett. **117**, 190601 (2016).

[17] N. Shiraishi and K. Saito, Fundamental relation between entropy production and heat current, J. Stat. Phys. **174**, 433 (2019).

[18] A. C. Barato and U. Seifert, Thermodynamic uncertainty relation for biomolecular processes, Phys. Rev. Lett. **114**, 158101 (2015).

[19] T. R. Gingrich, J. M. Horowitz, N. Perunov, and J. L. England, Dissipation bounds all steady-state current fluctuations, Phys. Rev. Lett. **116**, 120601 (2016).

[20] T. R. Gingrich, G. M. Rotskoff, and J. M Horowitz, Inferring dissipation from current fluctuations, J. Phys. A: Math. Theor. **50**, 184004 (2017).

[21] A. Dechant and S.-i. Sasa, Fluctuation-response inequality out of equilibrium, Proc. Natl. Acad. Sci. USA **117**, 6430 (2020).

[22] N. Shiraishi, Optimal thermodynamic uncertainty relation in Markov jump processes, J. Stat. Phys. **185**, 19 (2021).

[23] A. Dechant and S.-I. Sasa, Continuous time-reversal and equality in the thermodynamic uncertainty relation, Phys. Rev. Res. **3**, L042012 (2021).

[24] C. Dieball and A. Godec, Direct route to thermodynamic uncertainty relations and their saturation, Phys. Rev. Lett. **130**, 087101 (2023).

[25] N. Shiraishi and K. Saito, Information-theoretical bound of the irreversibility in thermal relaxation processes, Phys. Rev. Lett. **123**, 110603 (2019).

[26] A. Kolchinsky, A. Dechant, K. Yoshimura, and S. Ito, Information geometry of excess and housekeeping entropy production. arXiv:2206.14599.

[27] K. Tomita and H. Tomita, Irreversible circulation of fluctuation, Prog. Theor. Phys. **51**, 1731 (1974).

[28] N. Ohga, S. Ito, and A. Kolchinsky, Thermodynamic bound on the asymmetry of cross-correlations, Phys. Rev. Lett. **131**, 077101 (2023).

[29] P. Glansdorff and I. Prigogine, *Thermodynamics Theory of Structure, Stability and Fluctuations* (Wiley, London, 1971).

[30] K. Tomita, H. Ohta, and H. Tomita, Irreversible circulation and orbital revolution hard mode instability in far-from-equilibrium situation, Prog. Theor. Phys. **52**, 1744 (1974).

[31] Y. Kuramoto, *Chemical Oscillations, Waves, and Turbulence* (Springer, Berlin, 1984).

[32] Y. Cao, H. Wang, Q. Ouyang, and Y. Tu, The free-energy cost of accurate biochemical oscillations, Nat. Phys. **11**, 772 (2015).

[33] A. C. Barato and U. Seifert, Coherence of biochemical oscillations is bounded by driving force and network topology, Phys. Rev. E **95**, 062409 (2017).

[34] T. Herpich, J. Thingna, and M. Esposito, Collective power: Minimal model for thermodynamics of nonequilibrium phase transitions, Phys. Rev. X **8**, 031056 (2018).

[35] C. Fei, Y. Cao, Q. Ouyang, and Y. Tu, Design principles for enhancing phase sensitivity and suppressing phase fluctuations simultaneously in biochemical oscillatory systems, Nat. Commun. **9**, 1434 (2018).

[36] C. del Junco and S. Vaikuntanathan, High chemical affinity increases the robustness of biochemical oscillations, Phys. Rev. E **101**, 012410 (2020).

[37] P. Kumar and G. Gangopadhyay, Energetic and entropic cost due to overlapping of Turing-Hopf instabilities in the presence of cross diffusion, Phys. Rev. E **101**, 042204 (2020).

[38] D. Zhang, Y. Cao, Q. Ouyang, and Y. Tu, The energy cost and optimal design for synchronization of coupled molecular oscillators, Nat. Phys. **16**, 95 (2020).

[39] A. Pérez-Cervera, B. Lindner, and P. J. Thomas, Isostables for stochastic oscillators, Phys. Rev. Lett. **127**, 254101 (2021).

[40] M. J. del Razo, M. Dibak, C. Schütte, and F. Noé, Multiscale molecular kinetics by coupling Markov state models and reaction-diffusion dynamics, J. Chem. Phys. **155**, 124109 (2021).

[41] L. Oberreiter, U. Seifert, and A. C. Barato, Universal minimal cost of coherent biochemical oscillations, Phys. Rev. E **106**, 014106 (2022).

[42] A. Kolchinsky, N. Ohga, and S. Ito, Thermodynamic bound on spectral perturbations. arXiv:2304.01714.

[43] P. Pietzonka, A. C. Barato, and U. Seifert, Affinity- and topology-dependent bound on current fluctuations, J. Phys. A: Math. Theor. **49**, 34LT01 (2016).

[44] J. Schnakenberg, Network theory of microscopic and macroscopic behavior of master equation systems, Rev. Mod. Phys. **48**, 571 (1976).

[45] N. G. van Kampen, *Stochastic Processes in Physics and Chemistry* (North-Holland, Amsterdam, 2007).

[46] J. S. van Zon, D. K. Lubensky, P. R. H. Altena, and P. R. ten Wolde, An allosteric model of circadian KaiC phosphorylation, Proc. Natl. Acad. Sci. USA **104**, 7420 (2007).

[47] L. Potvin-Trottier, N. D. Lord, G. Vinnicombe, and J. Paulsson, Synchronous long-term oscillations in a synthetic gene circuit, Nature (London) **538**, 514 (2016).

[48] K. Fan, O. Taussky, and J. Todd, An algebraic proof of the isoperimetric inequality for polygons, J. Wash. Acad. Sci. **45**, 339 (1955).